

# Improving the Shunt Active Power Filter Performance Using Synchronous Reference Frame PI Based Controller with Anti-Windup Scheme

Consalva J. Msigwa, Beda J. Kundy, and Bakari M. M. Mwinyiwiwa

**Abstract**—In this paper the reference current for Voltage Source Converter (VSC) of the Shunt Active Power Filter (SAPF) is generated using Synchronous Reference Frame method, incorporating the PI controller with anti-windup scheme. The proposed method improves the harmonic filtering by compensating the winding up phenomenon caused by the integral term of the PI controller.

Using Reference Frame Transformation, the current is transformed from  $a-b-c$  stationary frame to rotating  $0-d-q$  frame. Using the PI controller, the current in the  $0-d-q$  frame is controlled to get the desired reference signal. A controller with integral action combined with an actuator that becomes saturated can give some undesirable effects. If the control error is so large that the integrator saturates the actuator, the feedback path becomes ineffective because the actuator will remain saturated even if the process output changes. The integrator being an unstable system may then integrate to a very large value, the phenomenon known as integrator windup. Implementing the integrator anti-windup circuit turns off the integrator action when the actuator saturates, hence improving the performance of the SAPF and dynamically compensating harmonics in the power network. In this paper the system performance is examined with Shunt Active Power Filter simulation model.

**Keywords**—Phase Locked Loop (PLL), Voltage Source Converter (VSC), Shunt Active Power Filter (SAPF), PI, Pulse Width Modulation (PWM).

## I. INTRODUCTION

THE ever increasing use of power semiconductor switching devices in power supply for DC motors, computers and other microprocessor based equipment causes harmonics in electric power system. Harmonics may cause serious problems such as excessive heating of electric motors and malfunction of sensitive electronic gadgets. Filtering of harmonics can be effected by using either passive or active power filters. Traditionally, passive filters have been used for harmonic

mitigation purposes. Active filters have been alternatively proposed as an adequate alternative to eliminate harmonic currents generated by nonlinear loads as well as for reactive power compensation. Various control methods with various control strategies as discussed in [1]-[12], [13-14] were implemented for minimizing harmonics in the electric power network. However, to date the shunt active power filter is still extensively used. Active Power Filter consists of Voltage Source Converter operating at relatively high frequency to give the output which is used for cancelling low order harmonics in the power system network. With Shunt Active Power Filter, crucial part involves generation of the reference signal used to generate gating signals for the VSC. Fig. 1 shows Block Diagram of PWM Controlled VSC operated as APF.

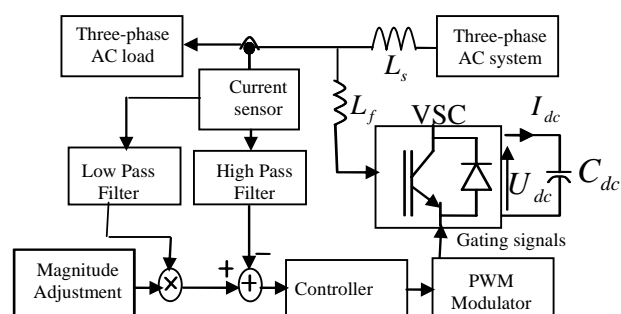


Fig. 1 Block Diagram of PWM Controlled VSC operated as APF

Several control methods involved in generating reference signals have been discussed in [1]-[12] among them being the Synchronous Reference Frame method. Many control strategies have been proposed, for example in [13]-[14] discussed about taking care of delays which when not taken care off, may cause the controller to be unstable hence the whole system becoming unstable. However where control is concerned, the integral component of the PI controller can lead to integrator windup resulting into instability of the controller and hence poor performance of the shunt active power filter. This paper presents a method to effectively compensate the windup of the integral term of the PI controller. It is an integrator anti-windup circuit.

C. J. Msigwa is with the Department of Electrical and Computer Systems Engineering, University of Dar es Salaam, Tanzania (phone: 0255-22-2410762; fax: 022-22-2410377/2410029; e-mail: msigwaj34@gmail.com).

B. J. Kundy is with the Department of Electrical and Computer Systems Engineering, University of Dar es Salaam, Tanzania (e-mail: bjkundy@udsm.ac.tz).

B. M. M. Mwinyiwiwa is with the Department of Electrical and Computer Systems Engineering University of Dar es Salaam, Tanzania (e-mail: bakary\_mwinyiwiwa@udsm.ac.tz).

An extra feedback path is provided by using output of the saturator model and forming an error  $e$  as the difference between the estimated actuator output  $u$  and the controller output  $c_u$  feeding this error back to the integrator through an appropriate gain. The error signal is zero when the actuator is not saturated. Emphasis is placed on choosing the gain, that it should be chosen large enough that the anti-windup circuit keeps input to the integrator small under all error conditions. The performance of the proposed method is examined with the Shunt Active Power Filter simulation model and the results are compared with the Shunt Active Power Filter without anti-windup scheme.

TABLE I  
NOMENCLATURE

|                                |  |
|--------------------------------|--|
| $L_s, L_f$                     | Line inductance, filter inductance                           |
| $I_{dc}, V_{dc}$               | dc current, dc. voltage                                      |
| $i_{liad}, i_{harmonics}$      | Load current, harmonics current                              |
| $i_{sa}, i_{sb}, i_{sc}$       | Three-phase currents   |
| $i_d, i_q$                     | Component currents in $dq$ - frame                           |
| $V_{aref}, V_{bref}, V_{cref}$ | Three-phase reference voltage                                |
| $K_p, K_i$                     | Proportional constant, integral constant                     |
| $e_s$                          | Error signal   |
| $u_c, u$                       | Controller output, actuator output                           |
| $T_i, T_t$                     | Integral time constant, tracking time constant               |
| $D_1, D_2$                     | Anti-parallel diodes   |
| $T_1, T_2$                     | Switches   |
| $p, n, z$                      | Positive rail, negative rail and neutral point respectively. |
| $\omega_0$                     | Target output frequency                                      |
| $\theta_0$                     | Arbitrary output phase                                       |

## II. HARMONIC CURRENT REFERENCE

To get the reference harmonic current, first the load current is measured. The load current consists of fundamental component  $i_1$  and harmonic component  $i_h$ . Using the band pass filter, with appropriate cut-off frequencies the fundamental current is extracted from the measured system load current. Using comparator, as shown in Fig. 2, the load current is compared with fundamental component and the error is the reference harmonics signal.

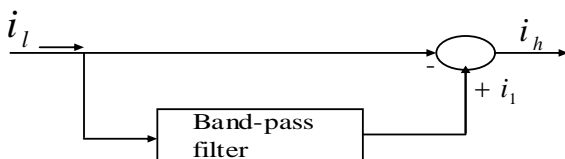


Fig. 2 Harmonic reference extraction

where  $i_h = \sqrt{i_{ha}^2 + i_{hb}^2 + i_{hc}^2}$ , the instantaneous magnitudes of the three phase harmonics current.  $i_l$  = load current and  $i_1$  = fundamental current.

## III. REFERENCE FRAME TRANSFORMATION

Reference frame transformation is the transformation of coordinates from a three-phase  $a-b-c$  stationary coordinates system to the  $0-d-q$  rotating coordinate system as shown in Fig. 3.

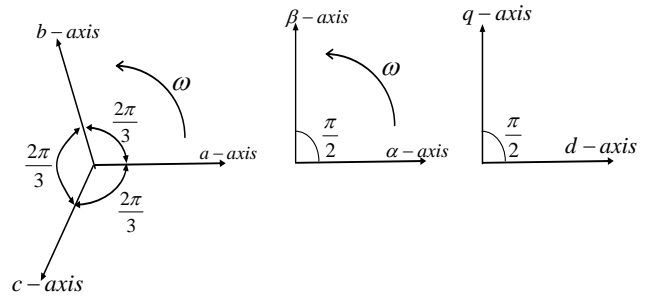


Fig. 3 Reference Frame Transformation

This transformation is important because it is in  $0-d-q$  reference frame the signal can effectively be controlled to get the desired reference signal. Transformation is made in two steps: First a transformation from the three-phase stationary coordinate system to the two-phase so-called  $0-\alpha-\beta$  stationary coordinate system is done. Load currents and voltages at Point of Common Coupling (PCC) are transformed into  $0-\alpha-\beta$  coordinates. The three-phase signal with maximum voltage  $V_m$ , at 120 degrees apart from each other is as given by (1):

$$f_{abc} = V_m \begin{bmatrix} \cos \omega t \\ \cos \left( \omega t - \frac{2\pi}{3} \right) \\ \cos \left( \omega t + \frac{2\pi}{3} \right) \end{bmatrix} \quad (1)$$

Fig. 4 shows the reference signal calculation for the PWM processes.

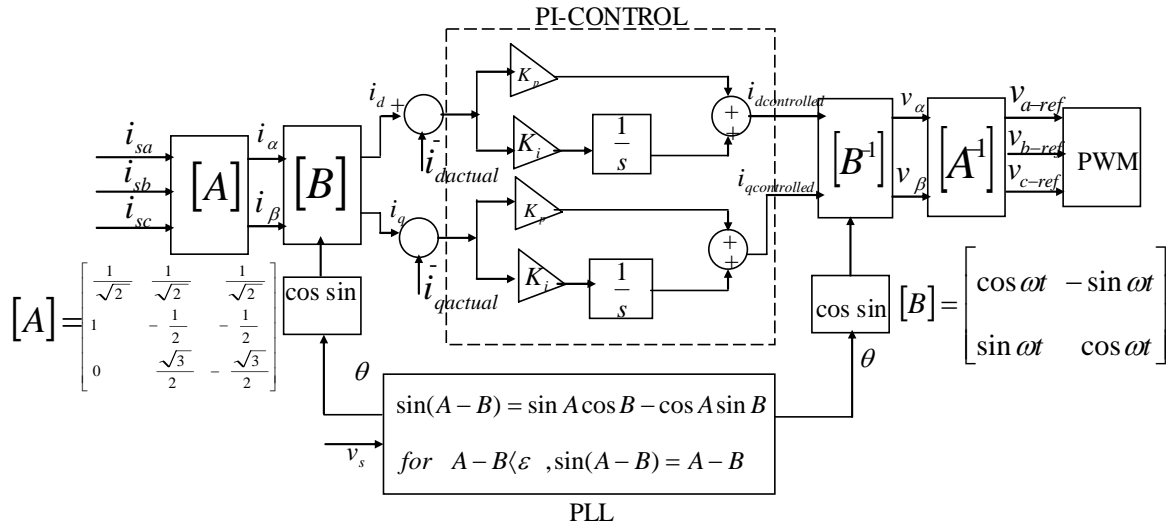


Fig. 4 Block diagram of reference signals calculation for the PWM

The signal  $f_{abc}$  in the  $a-b-c$  stationary frame is rotating with the frequency of  $\omega$  in radians /sec. The signals  $0-\alpha-\beta$  in stationary frame are obtained using (2).

$$f_{0\alpha\beta} = V_m \sqrt{\frac{2}{3}} \begin{bmatrix} \frac{1}{\sqrt{2}} & \frac{1}{\sqrt{2}} & \frac{1}{\sqrt{2}} \\ 1 & -\frac{1}{2} & -\frac{1}{2} \\ 0 & \frac{\sqrt{3}}{2} & -\frac{\sqrt{3}}{2} \end{bmatrix} \begin{bmatrix} \cos \omega t \\ \cos \left( \omega t - \frac{2\pi}{3} \right) \\ \cos \left( \omega t + \frac{2\pi}{3} \right) \end{bmatrix} \quad (2)$$

The axes,  $a$ ,  $b$ , and  $c$  are fixed on the same plane and are separated from each other by  $\frac{2\pi}{3}$  radians.  $0-\alpha-\beta$  are orthogonal axes with the  $\alpha$ -axis being synchronized with the  $a$ -axis of  $a-b-c$  plane and the  $\beta$ -axis being orthogonal to the  $\alpha$ -axis.  $f_{0\alpha\beta}$  in (2) is still rotating with the frequency of  $\omega$  radians/second. To eliminate this frequency, a step further is taken; a transformation from the  $0-\alpha-\beta$  stationary coordinate system to the  $0-d-q$  rotating coordinate system is performed. The matrix in (3):

$$[B] = \begin{bmatrix} \cos \omega t & \sin \omega t \\ -\sin \omega t & \cos \omega t \end{bmatrix} \quad (3)$$

is assigned such that when it is multiplied by  $f_{0\alpha\beta}$ , the  $0-\alpha-\beta$  coordinates which are in stationary frame will be rotating with the same frequency as that of  $0-d-q$  rotating

frame as given in (4):

$$f_{0dq} = \begin{bmatrix} \cos \omega t & \sin \omega t \\ -\sin \omega t & \cos \omega t \end{bmatrix} \begin{bmatrix} f_{0\alpha\beta} \end{bmatrix} \quad (4)$$

In synchronous reference frame-based controller, integrators are used to eliminate the steady state error of the DC component in the  $0-d-q$  frame of the reference signal. In accordance to the  $0-d-q$  frame theory, the current harmonics are represented as DC-components in their corresponding reference frame and the integrators eliminate the steady state error of each harmonic component. Using the Park transformation, reference signals are converted first into  $0-\alpha-\beta$  stationary frame, then into  $0-d-q$  rotating frame. The PI controller is used to eliminate the steady state error, and hence achieving the desired controlled reference signal. The algorithm is further carried a step forward, where the voltage reference signal in  $0-d-q$  rotating frame is converted back into  $a-b-c$  stationary frame, the reference signal for the Pulse Width Modulation (PWM). The inverse transformation from  $0-d-q$  rotating frame to  $a-b-c$  stationary frame is achieved using (5).

$$f_{abc} = [B^{-1}] f_{0dq} [A] \quad (5)$$

#### IV. THE PROPORTIONAL INTEGRAL (PI) CONTROLLER

The PI controller is very important part for the SAPF. It consists of proportional term and integral term. With this element, the best control performance of the SAPF is obtained. PI focuses on the difference (error) between the process variable (PV) and the set-point (SP), the difference between harmonics current reference signal  $i_h$  and the filter

current  $i_f$ . In this paper the PI controller has been implemented. PI controller algorithm involves two separate parameters; the Proportional and the Integral. The Proportional value determines the reaction to the current error; the Integral determines the reaction based on the sum of recent errors. The weighted sum of these two actions is used to adjust the process of the plant. By "tuning" the two constants in the PI controller algorithm, the PI controller can provide control action designed for specific process requirements. The textbook version control equation for the proportional plus integral (PI) is as given in (6) as expressed in [15].

$$u(t) = k_p e + k_i \int_{t_0}^t e(\tau) d\tau \quad (6)$$

With the controller transfer function as expressed in (7)

$$D_c(s) = k_p + \frac{ki}{s} \quad (7)$$

$k_p, k_i$  -are the proportional and integral gains.

The response of the controller can be described in terms of the responsiveness of the controller to an error, the degree to which the controller overshoots the set- point and the degree of system oscillation. Fig. 5 shows PI controller configuration.

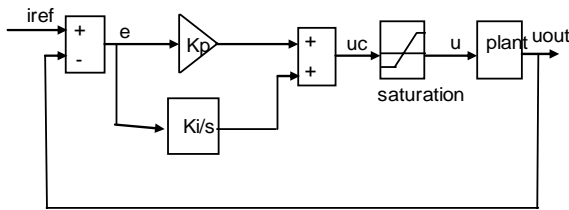


Fig. 5 PI controller without anti-windup scheme

#### A. Integrator Windup

A controller with integral action combined with the actuator that becomes saturated can give undesirable effects. If the controller error is so large that the integrator saturates the actuator, the feedback path will be broken because the actuator will remain saturated even if the process output changes. The integrator being unstable system may then integrate to a very large value. This effect is called integrator windup

There are several ways to avoid integrator windup. In this paper a method to effectively compensate the windup of the integral term of the PI controller is presented. A method for anti-windup is illustrated In Fig. 6. In this system an extra feedback path is provided by using the output of the actuator model and forming an error  $e_s$  as the difference between the estimated actuator output  $u$  and the controller output  $c_u$  and feeding this error back to the integrator through the gain  $1/T_t$

as shown in Fig. 6. The error signal  $e_s$  is zero when the actuator is not saturated. When the actuator is saturated the extra feedback tries to make the error signal  $e_s$  equal to zero. This means that the integrator resets so that the controller output is at the saturation limit. The integrator is thus reset to an appropriate value with the time constant  $T_t$ , which is called the tracking time constant.

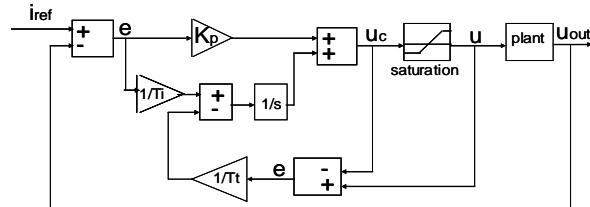


Fig. 6 PI controller with anti-windup scheme

When the control signal saturates, the integration state in the controller tracks the proper state. The tracking time constant  $T_t$  is the design parameter of the anti-windup. Common choices of  $T_t$  is as expressed in (8):

$$T_t = T_i \quad (8)$$

$T_i, T_t$  are the integral time constant and tracking time constants.

If  $0 < T_t \leq T_i$ , then the integrator state  $I(t)$  becomes sensitive to the instances when  $e_s \neq 0$ , as given in (9):

$$I(t) = \int_0^t \left[ \frac{Ke(\tau)}{T_i} + \frac{e_s(\tau)}{T_t} \right] d\tau \approx \frac{1}{T_t} \int_0^t e_s(\tau) d\tau \quad (9)$$

#### V. SINUSOIDAL PULSE WIDTH MODULATION (SPWM) SCHEME

SPWM scheme is used to determine the switching instants of the VSC for the purpose of maintaining Input/Output linearity especially for Active Power Filter applications. Fig. 7 shows the basic principle of SPWM as discussed in [16]. All modulation schemes in principle aim to create trains of switched pulses which have the same fundamental volt-second average (i.e. the integral of the voltage waveform over time) as a target reference waveform at any instant. There are several ways in which switching instants can be decided, at the same time maintaining the minimum harmonics content for the switched waveform. In this paper natural sampling is used, where the switching instants are determined by the intersection of the carrier waveform and the reference waveform. The more common form of naturally sampled PWM uses a triangular carrier instead of saw-tooth carrier to compare against the reference waveform.

Naturally sampled PWM compares a low frequency target

reference waveform  $V_{ref}$  (usually a sinusoid) against a high frequency carrier waveform  $V_{tri}$ . Fig. 7 shows one phase leg of an inverter driven by a triangular wave carrier. The phase leg is switched to the upper DC rail when the reference waveform is greater than the triangular carrier and to the lower DC rail when the carrier waveform is greater than the reference waveform.

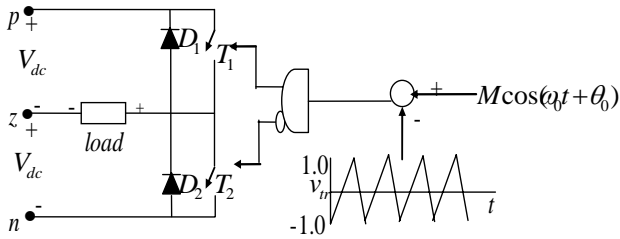


Fig. 7 Double-edge naturally sampled PWM with half bridge (one phase leg) voltage source converter

The reference waveform is expressed as:

$$v_{ref} = M \cos(\omega_0 t + \theta_0) = M \cos y \quad (10)$$

Where  $M$  = Modulation index or modulation depth (i.e., normalized output voltage magnitude) with range  $0 < M < 1$  and  $\omega_0$  = target output frequency.

Modulation index  $M$ , and number of pulses  $P$ , are expressed in (11) and (12).

$$M = \frac{\hat{u}_1}{u_d} \quad (11)$$

Where,  $\hat{u}_1, u_d$  - the peak of the fundamental-frequency component and dc input voltage, respectively.

Number of pulses,  $P$ , is given as in (11):

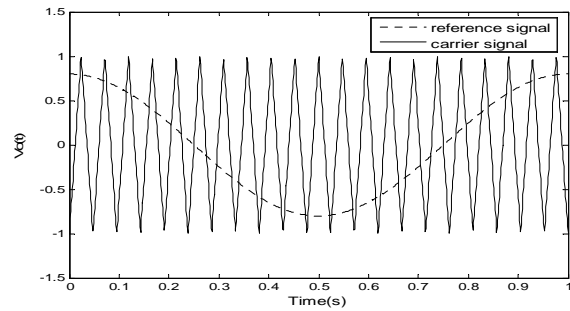
$$P = \frac{f_{sw}}{f_1} \quad (12)$$

where  $f_1, f_{sw}$ , are the fundamental frequency and switching frequency respectively.

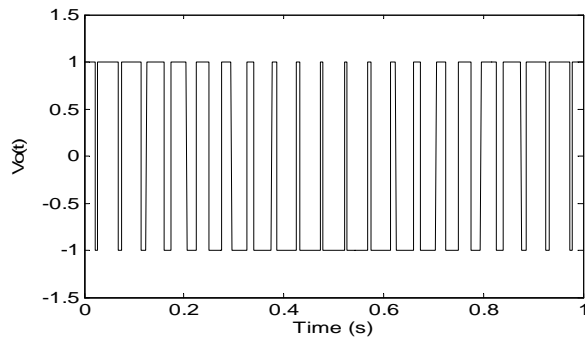
Carrier based method, causes low order harmonics due to processes such as over-modulation, when  $M \geq 1$  and the sampling process. During sampling processes all harmonics where harmonic number  $n$  is even are cancelled out between phase legs for all carrier/sampling combinations. But when the sawtooth carrier method or asymmetrical regular sampling is used, modulation process produces odd and even sideband harmonics around each carrier multiple. Significant odd sideband harmonics remain in the inverter output waveform around the odd carrier multiples despite harmonic cancellation between the phase legs. With triangular carrier method the effect for both natural sampling and asymmetrical regular

sampling is to totally cancel the sideband harmonics around the odd carrier multiples from the  $l-l$  waveform.[16]

MATLAB/SIMULINK software has been used to generate the switching signals. The triangular carrier method, natural sampling has been used. Simulation results for SPWM process is shown in Fig. 8. Fig. 8 (a) shows the comparison between the sinusoidal reference voltage with triangular carrier signal and Fig. 8 (b) shows the switching signals generated as a result of comparison between the carrier signal and reference signal.



(a)



(c)

Fig. 8 PWM Process

## VI. SIMULATION RESULTS

Simulations based on MATLAB/SIMULINK were implemented to verify the proposed Shunt Active Power Filter with anti-windup scheme. The circuit parameters of the equivalent power system based on Fig. 1 are as follows:  $V_{rms} = 380V$ ,  $V_{dc} = 450V$ ,  $L_s = 1.0 \text{ mH}$ ,  $L_f = 0.3 \text{ mH}$ . The power converter is switched at a frequency of 10 kHz. The 5<sup>th</sup>, 7<sup>th</sup>, and 11<sup>th</sup> harmonics were used to test the proposed Active Power Filter. Using Fast Fourier Transform (FFT), load current and source current were analyzed to obtain the Total Harmonic Distortion. Figs. 9-11 show the waveforms of the supply current before and after compensation, and the corresponding harmonic spectrums. The THD before compensation is 12.45%, after compensation using SAPF without anti-windup scheme is 4.40% and after compensation using SAPF with anti-windup scheme is 3.87%

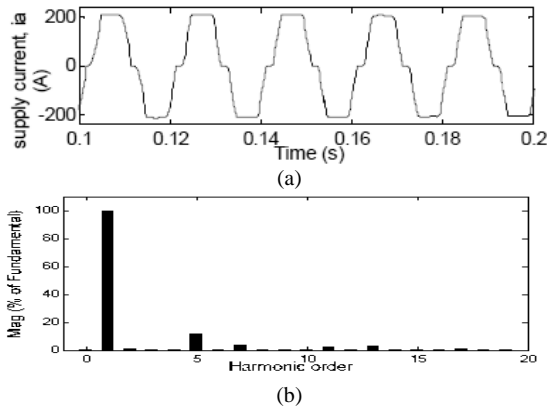


Fig. 9 (a) Source current before compensation, (b) Spectrum of source current before compensation (THD = 12.45%)

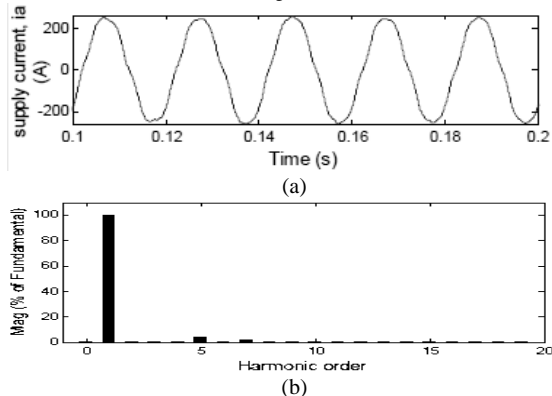


Fig. 10 (a) source utility current with active power filter without anti-windup, (b) Spectrum of supply current after compensation (THD=4.40%)

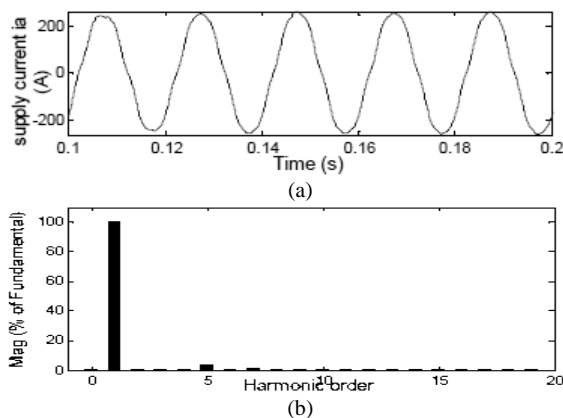


Fig. 11 (a) source utility current with active power filter with anti-windup, (b) Spectrum of supply current after compensation, (THD = 3.87%)

## VII. CONCLUSION

The Shunt Active power filter with SRF based-PI controller was examined in this paper. In rotating  $0-d-q$  frame, the SAPF with PI controller was modeled in two modes (i) without anti-windup circuitry, (ii) with anti-windup circuitry. The performance of the Shunt Active Power Filter with both

proposed controller circuit for reference current generation were examined with simulation model and the results were compared. The results show that with both algorithms the THD meets the recommended harmonic standards such as IEEE 519, where, the one with the anti-windup scheme achieved the best performance in terms of Active Filtering.

## ACKNOWLEDGMENT

The authors would like to acknowledge sida/SAREC for continued support.

## REFERENCES

- [1] Boon Teck Ooi, "Advanced Distribution to Deliver Custom Power", Electric Power Research Institute, Inc. (EPRI), 1991.
- [2] C. Qiao, K. M. Smedley, "Three-phase Active Power Filters with Unified Constant-frequency Integration control", [www.eng.uci.edu/~smedley/IPEMC-A185.PDF](http://www.eng.uci.edu/~smedley/IPEMC-A185.PDF).
- [3] C. Collombet, J. Lupin, J. Schonek, (1999), Harmonic disturbances in networks, and their treatment, Schneider Electric's "Collection Technique", Cahier technique no.152, [http://www.schneiderelectric.com/cahier\\_technique/en/pdf/ect202.pdf](http://www.schneiderelectric.com/cahier_technique/en/pdf/ect202.pdf). Available online.
- [4] U. Abdurrahman, R. Annette, L. S. Virginia, "A DSP Controlled Resonant Filter for Power Conditioning in Three-Phase Industrial Power", System. Signal Processing, Volume 82, Issue 11, November 2002, pp 1743-1752.
- [5] P. Fabiana, Pottker and B. Ivo, "Single-Phase Active Power Filters for Distributed Power Factor Correction", PESC 2000.
- [6] H.J. Gu, and H.C. Gyu, "New active power filter with simple low cost structure without tuned filters", 29th Annual IEEE Power Electronics Specialists Conference, Vol.1, pp 217-222, 1998.
- [7] F. Hideaki, Y. Takahiro, and A. Hirofumi, "A hybrid Active Filter for Damping of Harmonic Resonance in Industrial Power System", 29th Annual IEEE Power Electronics Specialists Conference, pp 209-216 1998.
- [8] M. Nassar, A. Kamal, D.A. Louis, "Nonlinear Control Strategy Applied to A Shunt Active Power Filter", Annual IEEE Power Electronics Specialists Conference, 2001.
- [9] M. Rukonuzzaman, and M. Nakaoka, "An Advanced Active Power Filter with Adaptive Neural Network Based Harmonic Detection Scheme, Annual IEEE Power Electronics Specialists Conference, 2001.
- [10] L. San-Yi, W. Chi-Jui, "Combined compensation structure of a static Var compensator and an active filter for unbalanced three-phase distribution feeders with harmonic distortion", Electric Power System Research 46, pp 243-250, 1998.
- [11] A. V. Stankovic, and T. A. Lipo, "A Generalized Control Method for Output-Input Harmonic Elimination for the PWM Boost Rectifier under Simultaneous unbalanced Input voltages and Input Impedances", Annual IEEE Power Electronics Specialists Conference, 2001.
- [12] Y. Ye, M. Kazerani, V. H. Quintana, "A Novel Modelling and Control Method for Three-Phase PWM Converters", Annual IEEE Power Electronics Specialists Conference, 2001.
- [13] C. Po-Tai, B. Subhashish, Dee pakraj M. Divan, "Hybrid parallel active/passive filter system with dynamically variable inductance" US Patent 1998
- [14] G. Marian, "Active Power Compensation of the current harmonics based on the instantaneous power theory" Department of electrical Engineering, Dunarea de Jos" University of Galati, Domneasca Street 47, 6200-Galati Romania
- [15] F. F. Gene, J. D. Powell, A. Emami-Naeini, Feedback Control of Dynamic system, Pearson Education. Inc. 1986, pp 186-190
- [16] D. G. Holmes T. Lipo, "Pulse width modulation for power converters-principles and practice" IEEE series on Power Engineering, pp 114-119, 2006.